

# $k_T$ -PINS RF Pulses for Low-Power Field Inhomogeneity-Compensated Multislice Excitation

Anuj Sharma<sup>1</sup>, Samantha Holdsworth<sup>2</sup>, Rafael O'Halloran<sup>2</sup>, Eric Aboussouan<sup>2</sup>, Anh Tu Van<sup>2</sup>, Julian Maclaren<sup>2</sup>, Murat Aksoy<sup>2</sup>, V Andrew Stenger<sup>3</sup>, Roland Bammer<sup>2</sup>, and William A Grissom<sup>1</sup>

<sup>1</sup>Biomedical Engineering, Vanderbilt University, Nashville, Tennessee, United States, <sup>2</sup>Radiology, Stanford University, Stanford, California, United States, <sup>3</sup>Medicine, University of Hawaii, Honolulu, Hawaii, United States

**Introduction** Simultaneous multislice (SMS) acquisitions are of significant interest for scan time reduction, especially in functional MRI and diffusion-weighted imaging<sup>1,2</sup>. However, SMS acquisitions at ultra-high field strength will suffer from spatially-varying contrast and SNR due to flip angle inhomogeneity resulting from  $B_1^+$  inhomogeneity. Furthermore, at ultra-high field SAR will be a problem for multiband excitation pulses, since the SAR of a conventional SMS pulse increases at least linearly with the number of excited slices<sup>3,4</sup>. The problem of increased power deposition in multi-slice imaging has been recently addressed by the Power Independent of Number of Slices (PINS) technique<sup>4</sup>. In this work we propose a new class of patient-tailored multiband excitation pulses, called  $k_T$ -PINS, that combines PINS with  $k_T$ -points<sup>5</sup> tailored RF pulses to overcome  $B_1^+$  inhomogeneity in SMS acquisitions at ultra-high field, without high SAR.

**Theory**  $k_T$ -PINS pulses are developed by capitalizing on the fact that both PINS and  $k_T$ -points pulses comprise trains of phase- and amplitude-modulated hard pulses that are separated by gradient blips. Thus, PINS pulses, which conventionally only deposit energy at discrete points along the  $k_z$  dimension in excitation k-space, can be augmented by introducing additional RF and gradient pulses that visit additional locations in the transverse ( $k_x$ - $k_y$ ) plane. This is illustrated in Fig. 2a. To design the  $k_T$ -PINS pulses we have extended a previously-described algorithm for parallel transmit spokes pulse design<sup>6</sup> to this problem. The inputs to the algorithm comprise the 3D  $B_1^+$  and  $B_0$  maps measured over the volume containing the slices, and a 3D target excitation pattern containing the target slice profiles. Note that even though the target pattern is specified over a limited FOV in the slice-dimension, the designed pulses will excite slices extending infinitely in  $z$ . The algorithm, illustrated in Fig. 1, starts with a hard pulse at DC, then adds new hard pulses and gradient blips on either side of that pulse using a greedy algorithm, until a desired total number of subpulses is reached. Between each subpulse addition, the RF weights, target excitation phase, and  $(k_x, k_y, k_z)$  locations of the subpulses are jointly optimized using a local descent-based algorithm.

**Methods** Single-channel excitation experiments were performed in a  $\text{CuSO}_4$  ball phantom to compare the proposed  $k_T$ -PINS pulses to conventional PINS pulses on a 7T Philips Achieva Scanner (Philips Healthcare, Cleveland, Ohio, USA). 3D  $|B_1^+|$  and  $B_0$  field maps were measured over a  $23 \times 23 \times 12$  cm FOV with a  $64 \times 64$  matrix size. A conventional PINS pulse was then designed to excite slice profiles with time-bandwidth product of 3, thickness 5 mm, and slice separation 35 mm. The PINS pulse had 21 total subpulses of 50  $\mu\text{s}$  duration each. A  $k_T$ -PINS pulse with 55 subpulses was then designed to produce the same excitation pattern, incorporating the measured  $B_1^+$  and  $B_0$  maps. The maximum gradient amplitude and slew rate were set to 40 mT/m and 150 mT/m/ms, respectively. Two identically parameterized scans were performed, one with each pulse, with FOV = 23 cm isotropic,  $128 \times 128$  matrix size and TE/TR of 10/200 ms. The flip angle variance was computed in each excited slice by dividing out the receive sensitivity from the acquired images, where the receive sensitivity was measured by acquiring a 3D low angle gradient echo image of the phantom and dividing out the measured  $|B_1^+|$  map. In addition, simulated excitation pattern predictions were used to compare the RF power deposited by  $k_T$ -PINS pulses to multiband (MB) spokes pulses<sup>7</sup>. Both pulses had time-bandwidth 2 and were designed to excite 3 slices of thickness 4 mm and 30 mm apart.

**Results** Figure 2 shows the designed pulses and the results of the phantom experiment. The three excited slices in the  $k_T$ -PINS experiment have a flip angle variance that is more than 30% lower than that for conventional PINS. Figure 3 illustrates  $k_T$ -PINS and multiband spokes pulses.  $k_T$ -PINS with 21 subpulses achieved 2.5 times less power deposition than the multiband spokes and a flip angle standard deviation of 3.7 degrees compared to 4.7 degrees for the spokes pulse.

**Conclusion** The proposed pulse is the first to enable multiband patient tailored imaging.

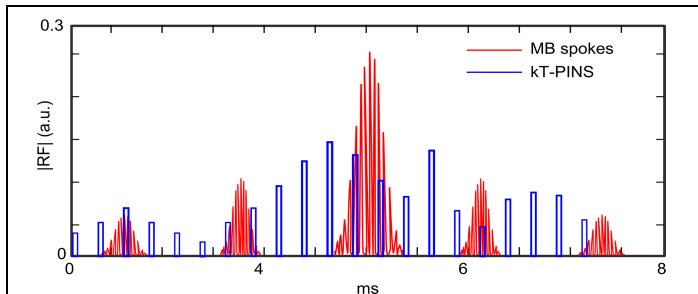


**Figure 3:** Comparison of multiband (MB) spokes and  $k_T$ -PINS pulses. The two pulses excite the same slice patterns, but the  $k_T$ -PINS pulse has 2.5x lower power.

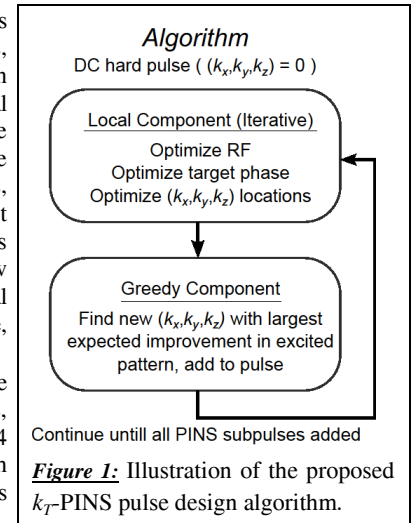


**Figure 1:** Illustration of the proposed  $k_T$ -PINS pulse design algorithm.

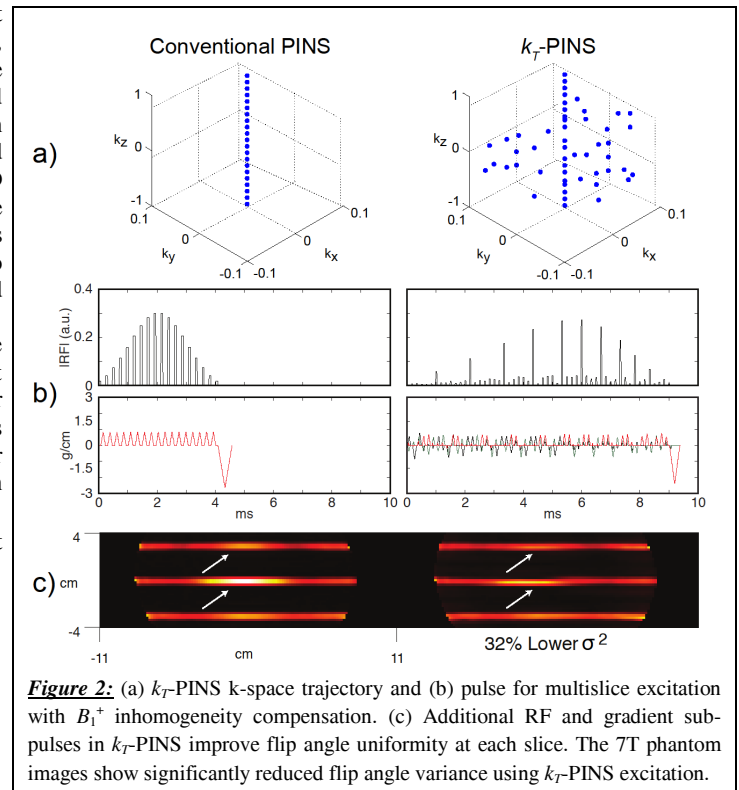


**Figure 2:** (a)  $k_T$ -PINS k-space trajectory and (b) pulse for multislice excitation with  $B_1^+$  inhomogeneity compensation. (c) Additional RF and gradient subpulses in  $k_T$ -PINS improve flip angle uniformity at each slice. The 7T phantom images show significantly reduced flip angle variance using  $k_T$ -PINS excitation.

**References** [1] D. A. Feinberg et al, PLoS ONE, Volume 5, Issue 12, 2010. [2] Larkman et al, MRM, 13:313-317, 2001. [3] E. Wong, ISMRM 2012, p. 2209. [4] D. G. Norris et al, MRM, 66:1234-1240, 2011. [5] M. A. Cloos et al, MRM, 67:72-80 (2012). [6] W. A. Grissom et al, MRM, 68:1553-1562, 2012. [7] A. Sharma et al, ISMRM 2013.